

Vertically aligned multi-layered structures to enhance mechanical properties of chitosan–carbon nanotube films

Minju Oh · Fangfang Sun · Hee-Ryung Cha · Jieun Park · Junggoo Lee ·
Moojin Kim · Kyoung-Bo Kim · Soo Hyung Kim · Jaebeom Lee ·
Dongyun Lee

Received: 26 September 2014 / Accepted: 29 December 2014 / Published online: 22 January 2015
© Springer Science+Business Media New York 2015

Abstract Pure chitosan and carbon nanotube (CNT)/chitosan nanocomposite films were fabricated via a sublimation-drying process at $-196\text{ }^{\circ}\text{C}$, during which polymeric repulsion generates unique pores with multi-layered structures. The films were then transformed into multi-layered and vertically aligned multi-layered (VAM) structures by compression. Due to the cross-linking between

layers, the films prepared at $-196\text{ }^{\circ}\text{C}$ showed significantly better mechanical properties than the films prepared at -78 and $-20\text{ }^{\circ}\text{C}$. Furthermore, a peculiar phenomenon was observed in that pure chitosan which exhibited better mechanical properties than the nanocomposites. To explain these results, we suggest a model in which the VAM structure supports more load than the CNT fillers.

Minju Oh and Fangfang Sun have contributed equally to this work.

M. Oh · J. Park · J. Lee (✉)
Department of Cogno-Mechatronics Engineering, Pusan National University, Busan 609-735, Republic of Korea
e-mail: jaebeom@pusan.ac.kr

F. Sun
Department of Biomedical Engineering, College of Life Information Science and Instrument Engineering, Hangzhou Dianzi University, Hangzhou 310018, China

H.-R. Cha · J. Lee
Powder & Ceramics Department, Korea Institute of Machinery & Materials, 66, Sangnam-dong, Changwon, Gyeongsangnam-do 641-831, Republic of Korea

M. Kim
POSCO Technical Research Laboratories, Songdo-dong, Yeonsu-gu, Incheon-si 406-840, Republic of Korea

K.-B. Kim
Center for Resources Information & Management, Korea Institute of Industrial Technology, 322 Teheran-ro, Gangnam-gu, Seoul 135-918, Republic of Korea

S. H. Kim · D. Lee (✉)
Department of NanoEnergy Engineering, Pusan National University, Busan 609-735, Republic of Korea
e-mail: dlee@pusan.ac.kr

Introduction

The outstanding properties of carbon nanotubes (CNTs) have been intensively studied, and, if used as a filler material in nanocomposites, they have normally been found to induce an improvement in the mechanical, thermal, and electrical properties of the original material [1–3]. The key point of composite technology is to transfer the favorable properties of the CNTs to the matrix by an unequivocal combination of two distinctive materials. Although significant advances have been made in recent years to overcome difficulties in the manufacture of polymer composites, the key challenge still remains in fully utilizing the properties of the nanoscale reinforcement. For example, many approaches take advantage of van der Waals interactions between the polymer matrix and the CNTs, since these methods preserve the properties of CNTs. Disadvantages may arise because of the weak force between wrapped/coupled molecules of two species that may lower the load transfer in the composites [4]. Moreover, the proper dispersion of the CNTs is the primary difficulty in achieving a nanoscale composite. The dispersion of the CNTs in a polymer matrix is essential for achieving the ultimate performance of a composite material, as nanotube aggregates tend to act as defect sites and

limit the composite's mechanical performance [5, 6]. Therefore, mixing CNTs in a polymer matrix always require special care in order to fully enhance the mechanical properties of polymeric materials.

Chitosan, because of its superb biocompatibility and film-forming ability, is a widely used polymer matrix in various fields, such as water treatment, separation membranes, food packaging, tissue engineering, and drug delivery [7–11]. Enhancing the mechanical properties of chitosan could broaden the range of applications in the fields mentioned above. We have previously reported two unique methods to prepare chitosan/CNT nanocomposite films, namely, sublimation-assisted compression (SAC) and the casting-evaporation method [12, 13]. It was reported that the mechanical properties, especially the ductility of chitosan-based nanocomposite films fabricated by the SAC method, were surprisingly improved owing to the well-dispersed CNTs. Additionally, more regular and porous microstructures were observed with lower fabrication temperatures. Based on these previous results, our current work thoroughly examines how the processing temperature affects the microstructure, and how controlling the microstructure influences the mechanical properties of pure chitosan and chitosan/CNT nanocomposites. By lowering the processing temperature, we observed more regular microstructures, and we discuss how the microstructures formed and affected the mechanical properties of pure chitosan and CNT/chitosan nanocomposites.

Experimental details

Commercially available multi-walled CNTs (MWCNT Co. LTD., Incheon, Korea) were used as filler materials in the fabrication of CNT/chitosan nanocomposites. The CNT modification and nanocomposite fabrication procedures were basically the same as those established in a previous study [12], with the exception of the fabrication temperature of the nanocomposites. In this study, the sublimation temperature, $-196\text{ }^{\circ}\text{C}$, was much lower than that in the previous work in which it was $-78\text{ }^{\circ}\text{C}$. To produce the CNT/chitosan nanocomposites, a water-based solution with surface-treated CNTs was added into a 1.0 wt% chitosan solution. The mixture was vigorously stirred with a magnetic bar for 2 h at the ambient temperature, followed by ultrasonic agitation for another hour, until no precipitation or aggregation was observed. The volume of the CNT solution was adjusted to 20 or 30 mL, such that the actual weight ratios of chitosan to CNT were $1:3.1 \times 10^{-3}$ (hereafter referred to as CNT1) and $1:4.7 \times 10^{-3}$ (hereafter referred to as CNT2), respectively, as shown in Table 1.

Preparation of films in liquid nitrogen

The pure chitosan and CNT/chitosan nanocomposite films were formed in liquid nitrogen at $-196\text{ }^{\circ}\text{C}$. The prepared pure chitosan and CNT/chitosan mixtures were cast in a Petri dish and carefully placed into liquid nitrogen for 10 min. The solidified pure chitosan and CNT/chitosan mixtures at $-196\text{ }^{\circ}\text{C}$ were immediately transferred into a freeze-dryer with a preset temperature of $-88\text{ }^{\circ}\text{C}$ and a pressure of 0.120 mbar for 120 h. Finally, the obtained foam-type pure chitosan and CNT/chitosan nanocomposites were pressed into a flexible thin film by an applied load of 10 tons for 10 s at ambient temperature. To observe the cross-sectional views, the specimens were carefully cut by razor blades.

Mechanical properties of the films

The mechanical properties of the pure chitosan and nanocomposite films were carefully investigated using a tensile tester (LRXPlus, Lloyd Instruments, UK), and a nanoindentation system (G200TM, Agilent Tech. USA). The detailed testing methodology for the tensile and nanoindentation tests can be found elsewhere [12]. More than 20 specimens in each condition were tested for understanding tensile properties. For the nanoindentation experiments, a three-sided pyramidal (Berkovich-type) diamond tip was used, and an indentation strain rate of 0.05 s^{-1} was adopted for a predetermined load, followed by a constant load dwell time of 10 s [14, 15]. The subsequent unloading was performed at the same strain rate. In order to avoid substrate effects, the indentation depth was limited to 20 % of the composite film thickness. The indentation displacement data were averaged from at least 30 indentations with the standard deviation indicating scatter in the displacement.

Results and discussion

Microstructures in cross-sectional and plane-view (insets) of pure chitosan and CNT/chitosan nanocomposites fabricated at $-196\text{ }^{\circ}\text{C}$ are shown in Fig. 1a–c. Cross-sectional images of pure chitosan and CNT/chitosan nanocomposites fabricated at $-78\text{ }^{\circ}\text{C}$ from our previous studies are also included in Fig. 1d and e for comparison [12]. Plane-view of CNT/chitosan nanocomposites fabricated in $-196\text{ }^{\circ}\text{C}$ after removing a layer is shown in Fig. 1f. One could clearly see that uniform distribution of CNTs in chitosan matrix. Compared with the specimens fabricated at $-78\text{ }^{\circ}\text{C}$, pure chitosan and the CNT/chitosan nanocomposites prepared at $-196\text{ }^{\circ}\text{C}$, show unique structures that are regularly aligned in the vertical direction. These vertically aligned multi-layered (VAM) structures, in the

Table 1 Chitosan/CNT weights in the investigated nanocomposites

CNT/chitosan nanocomposite films	Chitosan (g)	CNT (mg)	Chitosan/CNT w/w ratio
CNT1/chitosan	0.5	1.55	1/0.0031
CNT2/chitosan	0.5	2.33	1/0.0047

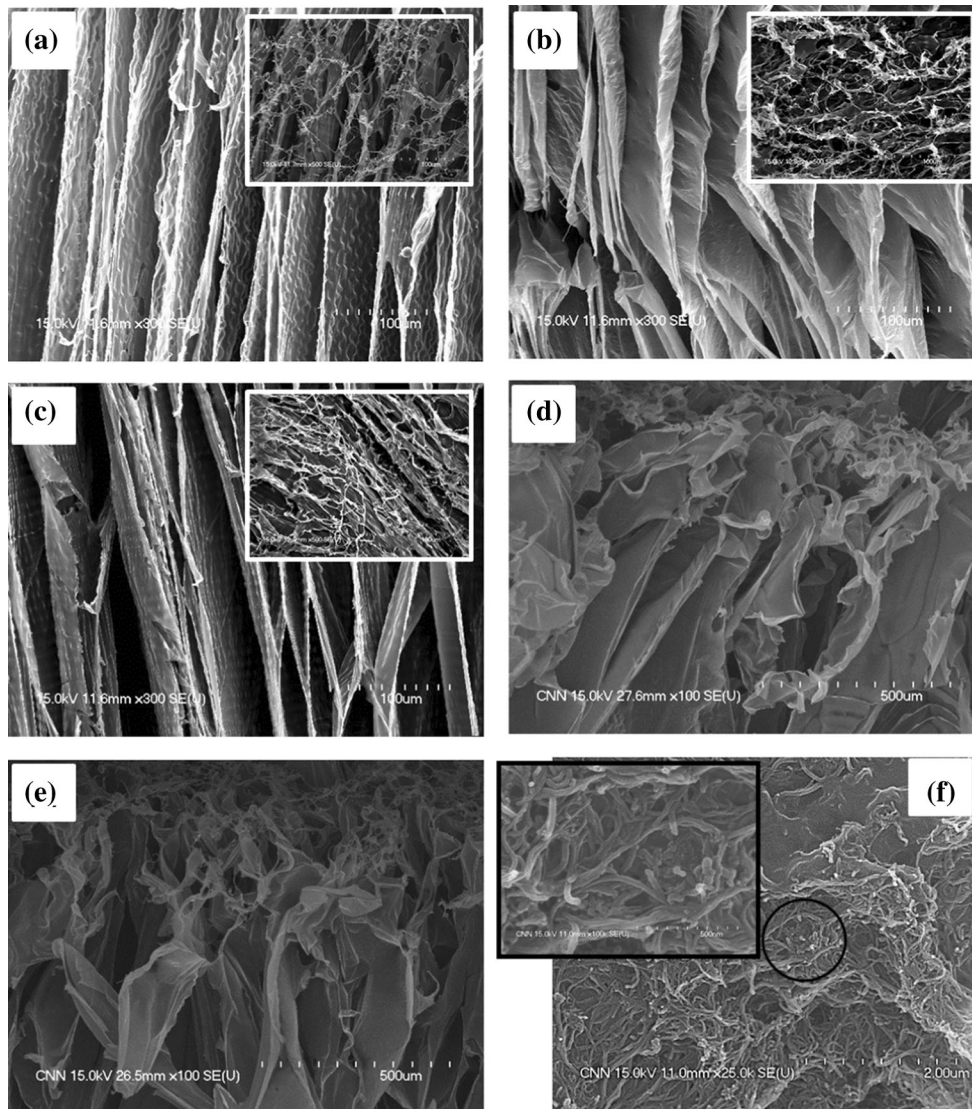


Fig. 1 Cross-sectional and plane-view (*insets*) SEM images of **a** pure chitosan specimens, **b** CNT1/chitosan nanocomposites, and **c** CNT2/chitosan nanocomposites at $-196\text{ }^{\circ}\text{C}$. For comparison, **d** pure

chitosan specimen at $-78\text{ }^{\circ}\text{C}$ and **e** CNT1/chitosan nanocomposites at $-78\text{ }^{\circ}\text{C}$ are shown

cross-sectional view, are attributed to the heat flow direction during solidification in the fabrication process of the foamed chitosan structures (Fig. 1a in Ref. [13]). Due to the physical and chemical responses of the nanocomposite components to heat, homogeneous and rapid heat transfer

in the solidification process may be essential in obtaining optimized nanocomposites. Therefore, polymer rheology may dominate the microstructure of composite films, regardless of nanofiller materials. It seems that the most important factor in the SAC method could be

thermodynamical variance, i.e., the temperature change during the freezing-sublimation process. A larger change of temperature during sublimation might afford a highly directional heat flow which induces the formation of regular microstructures.

The insets in Fig. 1a–c are plane-view images of the porous chitosan and CNT/chitosan nanocomposites. Interestingly, submicron-sized string-like structures covered the surfaces of both pure chitosan and the CNT/chitosan nanocomposites. These string-like structures may be remnant chitosan polymer chains from the sublimation process, rather than CNT-related structures, as the microstructures of pure and CNT-added porous chitosan composites do not differ greatly in both plane- and cross-sectional views. One could imagine that CNTs may affect the microstructure of porous chitosan, but according to our present observations, this assumption might be acceptable only in the case of a fabrication temperature higher than $-196\text{ }^{\circ}\text{C}$, i.e., at $-78\text{ }^{\circ}\text{C}$ (Fig. 1d, e) and $-20\text{ }^{\circ}\text{C}$. In Fig. 1d and e, relatively distinctive microstructures of porous chitosan, with and without CNTs, have been observed [12]. Additionally, the lamella-like structures in the cross-sectional view aligned more regularly after the addition of CNTs at $-78\text{ }^{\circ}\text{C}$, while such highly ordered lamella-like structures could be found in both pure chitosan and CNT/chitosan nanocomposites fabricated at $-196\text{ }^{\circ}\text{C}$.

It is plausible that the thermal effect of using different fabrication temperatures may be a dominant factor in the production of the microstructure. Let us define a given temperature for the SAC process and a freezing temperature of free movement of the polymer in the solvent as T_{SAC} and T_{POL} , respectively. Presumably, when T_{SAC} is lower than T_{POL} , the thermal properties of polymer matrix will be sustained even though the filler materials were included inside the polymer matrix. However, the ratio of polymer/nanofiller may also be important in a certain range, and may directly influence the mechanical properties of nanocomposite films.

To investigate the mechanical properties of the inorganic filler materials, the mechanical properties of the fabricated porous chitosan and different ratios of CNT/chitosan nanocomposites, which were compressed to obtain multi-layered structures, were obtained by tension and nanoindentation tests and the results are shown in Fig. 2a and b, respectively. Yield strength, ultimate tensile strength, elastic modulus, and elongation at fracture are listed in Table 2. As shown in Table 2 and Fig. 2a, the CNT1/chitosan nanocomposite showed the highest elastic modulus and yield strength of about 3.2 and 13 MPa, respectively. Further addition of CNTs (150 % more CNT was added in the CNT2/chitosan film than the CNT1/chitosan film) did not enhance the modulus and yield strength, as indicated by the CNT2/chitosan data. However,

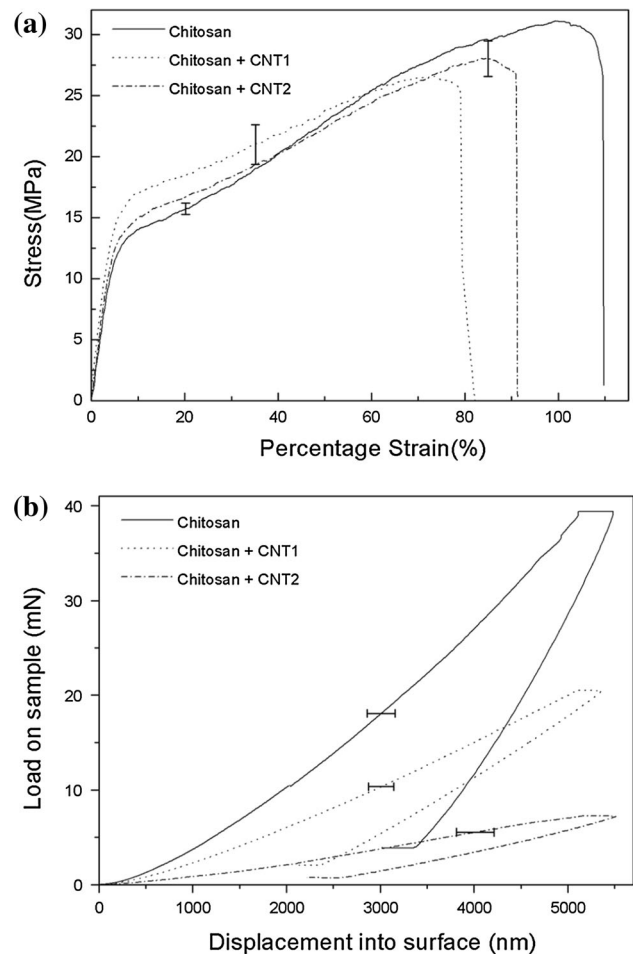


Fig. 2 **a** Tension and **b** nanoindentation results of chitosan and CNT/chitosan nanocomposites with different amounts of CNTs

Table 2 Mechanical properties, i.e., young's modulus (E), yield strength (σ_y), ultimate tensile strength, and elongation at fracture (ϵ_f), derived from tensile tests of pure chitosan and CNT/chitosan nanocomposites

	E (GPa)	σ_y (MPa)	UTS (MPa)	ϵ_f (%)
Pure chitosan	2.68	9.64	31.12	109.63
CNT1/chitosan	3.21	12.98	26.56	79.40
CNT2/chitosan	2.95	10.45	28.06	91.25

the addition of CNTs did enhance the mechanical properties with regard to pure chitosan, especially in yield strength. Therefore, it could be concluded that a certain amount of CNTs do play a positive role in enhancing the mechanical properties. However, it is noticeable that pure chitosan showed a higher ultimate tensile strength and elongation than the CNT/chitosan nanocomposites, with typically about 17 % higher ultimate tensile strength and 38 % higher elongation. The noticeable mechanical

strength of the chitosan film may result in unique VAMS structure through the SCA method. As such, nanoindentation has been adopted for understanding the mechanical behavior of the nanocomposites. As shown in Fig. 2b, load–displacement curves of the specimens showed that pure chitosan sustains a much higher load at the same displacement than the CNT/chitosan nanocomposites. Typically, at a depth of 4000 nm, pure chitosan held almost a five times higher load than the CNT2/chitosan nanocomposites. The nanoindentation results are in good agreement with the results of the tensile tests; for example, CNT2/chitosan nanocomposites sustained much lower load than the CNT1/chitosan nanocomposites. The unloading curvature of the specimens shows its ability to resist a change in shape (stretching, bending, or twisting) or stiffness. Multi-layered pure chitosan specimens showed a much higher stiffness than CNT-added chitosan nanocomposites; however, those nanocomposites have a better recovery characteristic or high resilience, the capacity of a material to absorb energy when it is deformed elastically. CNT2/chitosan nanocomposites show the lowest load-sustaining capacity in nanoindentation tests, but a higher ultimate tensile strength than CNT1/chitosan nanocomposites. A nanoindentation test shows the local properties of how CNTs interact with chitosan chains to enhance the mechanical properties of the material, whereas a tension test represents the overall properties of the nanocomposites. Furthermore, in the VAM structure, the direction of indentation or tension will be closely related to the mechanical strength of the microstructures, which will be discussed later.

For further comparison, the stress–strain curves of pure chitosan and CNT1/chitosan nanocomposites fabricated at -78 and -196 °C are shown in Fig. 3. Specimens

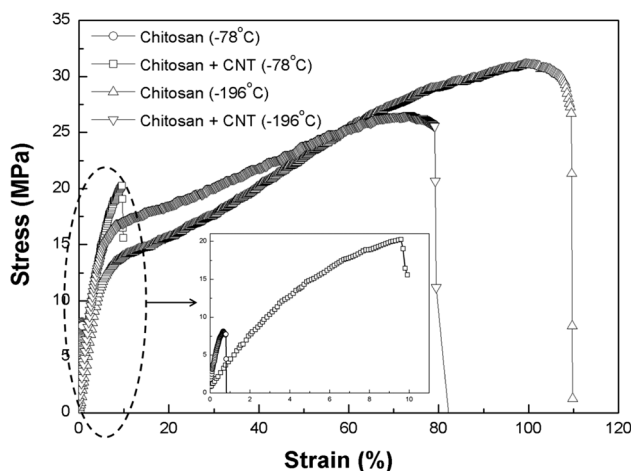


Fig. 3 Stress–strain curves of pure chitosan and CNT1/chitosan nanocomposites fabricated at -78 and -196 °C. The inset shows an enlarged graph of the specimen fabricated at -78 °C

fabricated at -196 °C revealed up to about 100 times higher strain and four times enhanced tensile strength. Note that the addition of CNTs into the chitosan matrix affected the properties of the resulting nanocomposites in a completely different manner. The CNTs have a positive effect in case of specimens fabricated at -78 °C, but a relatively negative or no significant effect for the specimens fabricated at -196 °C, which is probably related to the differences between T_{SAC} and T_{POL} . We may assume that T_{POL} of chitosan might be lower than -78 °C for aqueous chitosan. Moreover, the kinetics of solidification in a given solvent may strongly depend on the processing temperature; it is probable that as the rate of solidification increases, the distribution of freezing energy becomes more homogenous. These results are presumably related to the fabrication of different microstructures that strongly depend on the processing temperature.

These interesting behaviors could be interpreted by a comprehensive consideration of the microstructures, test methods, and interaction between filler material and matrix through fracturing specimens without any further handling that may distort original mechanical information. Figure 4 shows representative fracture surfaces of three different specimens, in which the cross section shows a unique VAM structure, with some areas highlighted by white dotted circles for further consideration. While the fracture surface of pure chitosan clearly exhibits VAM structures shown in Fig. 4a, the CNT-added specimens exhibit a less regular, or partially collapsed, VAM structures between the pressed layers (see Fig. 4b, c). For better inspection, the magnified images of dotted area in Fig. 4a–c are presented in Fig. 4a'–c' showing a typical VAM structure. Regular VAM structures could act as load-sustaining component; therefore, better mechanical properties are surprisingly observed in pure chitosan rather than in the CNT/chitosan nanocomposites.

Figure 5 is a schematic diagram illustrating the formation of the VAM structure and the role of CNTs. CNTs may act as defects by blocking the connection between layers of polymeric chains and form truss structures. The most efficient way to make reactive CNTs as a filler material is to introduce some functional groups on the CNT surface, such as carboxylic or hydroxyl groups. In the present case, the CNTs were preserved by an acidic treatment, specifically by refluxing with concentrated nitric acid before the experiment to enhance the interaction between the chitosan and CNTs. Therefore, CNTs were presumably wrapped by functional groups of chitosan and homogeneously blended within the chitosan matrix. The well-blended CNTs within the chitosan matrix possibly block the folding and connecting of chitosan chains from different layers that form the VAM structures. In the tensile tests, performed along with the direction parallel to the layers, the polymer chains

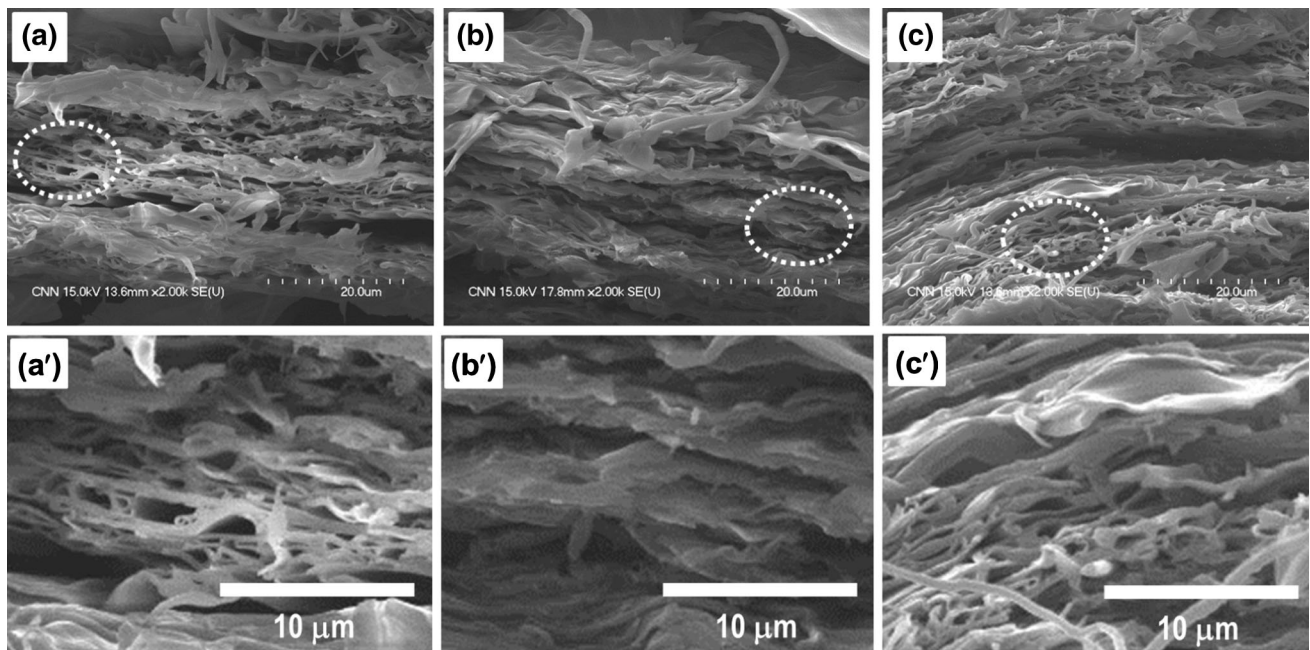
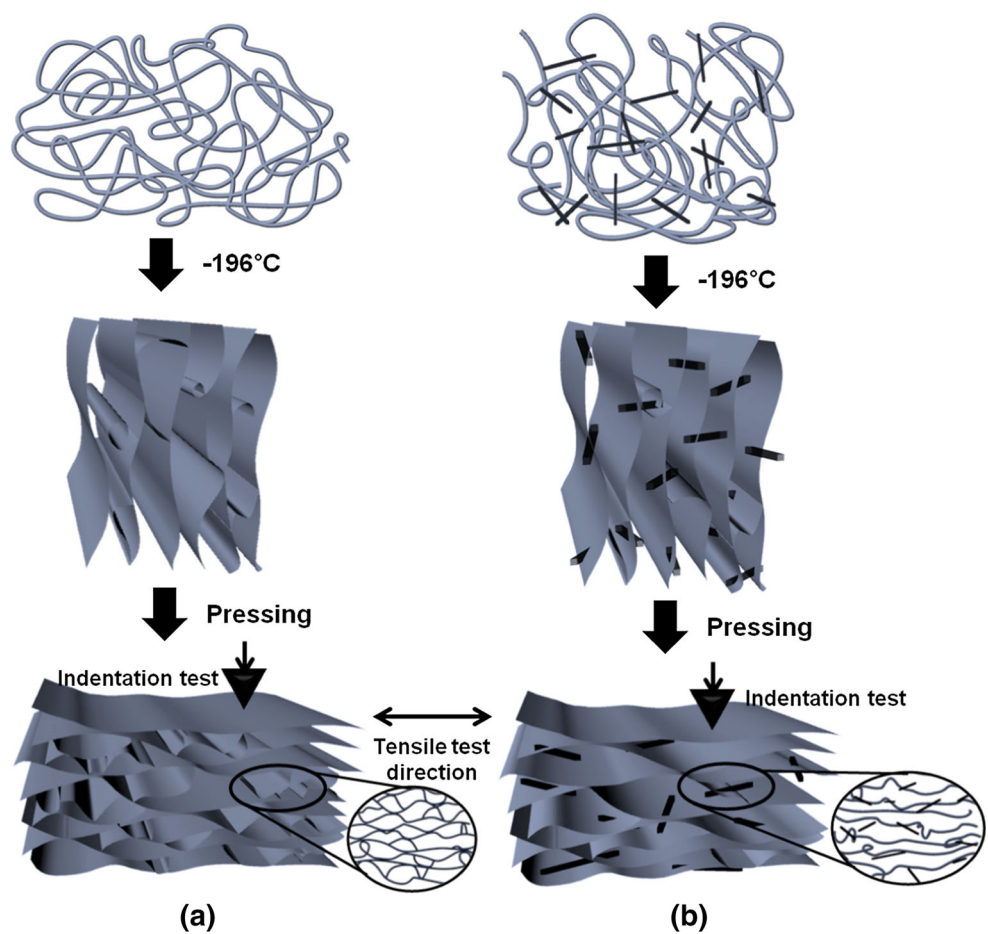


Fig. 4 SEM images of fracture surfaces after tensile tests: **a** pure chitosan, **b** CNT1/chitosan nanocomposites, **c** CNT2/chitosan nanocomposites. **a'–c'** Are the magnified images of *dotted area* in each specimen showing atypical VAM structure

Fig. 5 Schematics of the formation mechanism of multi-layered **a** pure chitosan and **b** CNT/chitosan nanocomposites employing the ultra-low temperature sublimation technique



attached between the layers could plastically deform at relatively low stress, while the VAM structure acts as stress-sustaining element after stretching, thus resulting in an ultimate enhancement of tensile stress. The stretching of the main polymer chains and VAM structure consequently leads to a large strain. In contrast, the addition of CNTs seems to disturb the formation of the VAM structure present in pure chitosan (see Fig. 3b, c). CNTs attached to the main polymer chains could improve the yield strength of the specimen at the initial stage of deformation, but with increasing load, the less uniform/incomplete VAM structures cannot support the higher stresses, resulting in a relatively low elongation. This is why the interpretation of the mechanical behavior of the specimens on the basis of nanoindentation tests was approached in a slightly different way, compared to the tensile tests (Figs. 2a, 3). The schematics at the bottom of Fig. 5 indicate the direction of the tensile and nanoindentation tests in this study. The dense VAM structures in pure chitosan specimens may be able to withstand a large compressive stress, whereas the relatively less dense VAM structures formed by the addition of CNTs may not withstand a compressive stress as high as that pure chitosan can resist. This schematic diagram may be based on qualitative analysis, but it is worthwhile to understand the roles of VAM and CNTs on the mechanical properties of this specific chitosan matrix.

Conclusion

An ordered structure of chitosan matrix was fabricated via a SAC process, in which polymeric repulsion and heat transfer generate a unique structure. The chitosan foam was then transformed into a multi-layered film by compression to produce a VAM structure. Due to the microscale-aligned stacking of cross-linked layers, the VAM-structured films prepared in liquid nitrogen showed significantly improved tensile strength and a remarkable flexibility compared to the films prepared at higher temperatures of -78 and -20 °C. A peculiar phenomenon was observed in tensile and nanoindentation tests: pure chitosan VAM films exhibited better mechanical properties than CNT-added VAM nanocomposites. A model explained that the CNT filler inhibits VAM structure formation in higher CNT weight ratio CNT/polymer nanocomposites.

Acknowledgements This research was co-supported by (1) the Basic Science Research Program through the National Research Foundation of Korea (NRF) funded by the Ministry of Education (NRF-2010-0025175), (2) a grant from the Fundamental R&D Program for Core Technology of Materials funded by the Ministry of Trade, Industry & Energy, Republic of Korea, (3) the Civil & Military Technology Cooperation Program through the National Research Foundation of Korea (NRF) funded by the Ministry of Science, ICT & Future Planning (No. 2013M3C1A9055407).

References

1. Curtin WA, Sheldon BW (2004) CNT-reinforced ceramics and metals. *Mater Today* 7:44–49
2. Salvat JP, Bonard JM, Thomson NH, Kulik AJ, Foró L, Benoit W, Zuppiroli L (1999) Mechanical properties of carbon nanotubes. *Appl Phys A* 69:255–260
3. Hou Y, Tang J, Zhang H, Qian C, Feng Y, Liu J (2009) Functionalized few-walled carbon nanotubes for mechanical reinforcement of polymeric composites. *ACS Nano* 3:1057–1062
4. Balasubramanian K, Burghard M (2005) Chemically functionalized carbon nanotubes. *Small* 1(2):180–192
5. Harris PJF (2009) Carbon nanotube science: synthesis, properties and applications. Cambridge University Press, Cambridge
6. Park JH, Alegaonkar PS, Jeon SY, Yoo JB (2008) Carbon nanotube composite: dispersion routes and field emission parameters. *Compos Sci Technol* 68:753–759
7. Harrison BS, Atala A (2007) Carbon nanotube applications for tissue engineering. *Biomaterials* 28:344–353
8. Liu Y, Wang M, Zhao F, Xu Z, Dong S (2005) The direct electron transfer of glucose oxidase and glucose biosensor based on carbon nanotubes/chitosan matrix. *Biosens Bioelectron* 21:984–988
9. Liu Y, Liu L, Dong S (2007) Electrochemical characteristics of glucose oxidase adsorbed at carbon nanotubes modified electrode with ionic liquid as binder. *Electroanal* 19(1):55–59
10. Xie F, Weis P, Chauvet O, Bideau JL, Tassin JF (2010) Kinetic studies of a composite carbon nanotube-hydrogel for tissue engineering by rheological methods. *J Mater Sci-Mater Med* 21:1163–1168. doi:10.1007/s10856-009-3984-x
11. Zhang M, Smith A, Gorski W (2004) Carbon nanotube–chitosan system for electrochemical sensing based on dehydrogenase enzymes. *Anal Chem* 76:5045–5050
12. Sun F, Cha HR, Bae K, Hong S, Kim JM, Kim SH, Lee J, Lee D (2011) Mechanical properties of multilayered chitosan/CNT nanocomposite films. *Mater Sci Eng, A* 528:6636–6641
13. Sun F, Lim BK, Ryu SC, Lee D, Lee J (2010) Preparation of multi-layered film of hydroxyapatite and chitosan. *Mater Sci Eng, C* 30:789–794
14. Lucas BN, Oliver WC (1999) Indentation power-law creep of high-purity indium. *Metall Mater Trans A* 30:601–610
15. Oliver WC, Pharr GM (1992) An improved technique for determining hardness and elastic-modulus using load and displacement sensing indentation experiments. *J Mater Res* 7:1564–1583